International Journal of Multiphase Flow 35 (2009) 792–800

Contents lists available at ScienceDirect

International Journal of Multiphase Flow

journal homepage: www.elsevier.com/locate/ijmulflow

Review

Two-way coupled turbulence simulations of gas-particle flows using point-particle tracking

John K. Eaton

Department of Mechanical Engineering, Stanford University, CA 94305, United States

ARTICLE INFO

Article history:
Received 6 July 2008
Received in revised form 14 February 2009
Accepted 19 February 2009
Available online 27 February 2009

Keywords:
Gas-particle flows
Turbulence
Large eddy simulation
Direct numerical simulation
Turbulence attenuation
Point-force coupling
Eulerian–Lagrangian

ABSTRACT

This paper addresses computational models for dilute gas-particle multiphase flow in which the three dimensional, time-dependent fluid motion is calculated in an Eulerian frame, and a large number of particles are tracked in a Lagrangian frame. Point forces are used to represent the back effect of the particles on the turbulence. The paper describes the early development of the technique, summarizes several experiments which show how dilute particle loadings can significantly alter the turbulence, and demonstrates how the point-particle method fails when the particles are comparable in scale to the small scale turbulence. High-resolution simulations and experiments which demonstrate the importance of the flow details around individual particles are described. Finally, opinions are stated on how future model development should proceed.

1. Introduction

Research on particle-laden multiphase flow at Stanford began in the early 1980s with an experiment on air flow through vertical diffusers located above a fluidized bed (Kale and Eaton, 1985). We found that the presence of a relatively dilute loading of particles in the diffuser profoundly affected the mean velocity field. The flow through a wide-angle diffuser was fully stalled in single-phase flow, but it was fully attached with the addition of a light loading of 75 μm diameter glass beads. This experiment is representative of a broad class of two-phase flows, namely gas flows with a dilute loading of fine solid particles. In such flows, the motion of the particles is controlled by the gas-phase flow with only minor affects of particle collisions with walls or other particles. At the same time, the particles can have a very strong effect on the gas-phase flow, even at particle volume fractions below 0.1%.

In trying to understand the diffuser results, we developed a code following the particle-source-in cell (PSIC) method published by Crowe et al. (1977). In this approach, the gas-phase motion is computed on a regular Eulerian grid, while Lagrangian calculations are done for the motion of representative particles taking account of the drag force of the gas on the individual particles. A simple, quasi-steady drag law, either Stokes flow or an empirical correlation is used to calculate the magnitude and direction of the drag force at each point along the particle trajectory. The "back-effect" of the particles on the gas flow is incorporated by calculating source terms for each computational volume. For example, a momentum source term is calculated by finding the net change in momentum of all particles passing through a given grid cell. A mass source term can be calculated similarly for evaporating droplets, etc.

Our model used the Reynolds-averaged Navier–Stokes (RANS) equations with a conventional single-phase turbulence model. Experiments[1] had shown that a dilute particle loading could drastically alter the turbulence statistics. However, there was no consensus on how to incorporate this effect into turbulence models. We believed this deficiency caused the failure of our model to accurately predict the diffuser flow. This launched our group at Stanford into a two-decade research effort combining experiments and simulations attempting to understand and model turbulence modification by dispersed solid particles. The simulation efforts have focused on incorporating point particles into direct numerical simulation (DNS) and large eddy simulation (LES) codes and on fully resolved simulations to understand how we can capture turbulence modulation effects in a point-particle simulation.

This paper provides a summary of research in our group on simulation of particle-laden turbulent gas flows. Some reference is made to the work of others, but this paper is not intended to be

[1] For an extensive review see article 12.6 by J.K. Eaton on Turbulence Modulation by Particles in Crowe, C.T., ed. *Multiphase Flow Handbook*, Taylor & Francis, Boca Raton, FL, 2006.

E-mail address: eatonj@stanford.edu

0301-9322/$ - see front matter © 2009 Elsevier Ltd. All rights reserved.
doi:10.1016/j.ijmultiphaseflow.2009.02.009

a comprehensive review of the field. The paper will first describe our early work on incorporating Lagrangian particle tracking and point-force two-way coupling into existing single-phase DNS and LES codes for homogeneous turbulent flows. I will next give a brief summary of experimental evidence for turbulence modification by particles, since prediction of this phenomenon has been the main focus of our subsequent simulation work. There will be an extensive discussion on the implementation of two-way coupling in simulations of realistic flows where the particle size may be comparable to single-phase grid scales. Finally, I will discuss simulations and experiments that resolve the flow around individual particles and discuss how these findings may be incorporated into future simulation models.

2. Homogeneous flow simulations

Our work on simulating particle-laden gas flows began with a study of inertial particles moving in homogeneous, isotropic turbulence. This work was motivated by the need for fluid velocity statistics measured along the path of an inertial particle for incorporation into models for turbulent particle dispersion and turbulence modification by particles. The simulations resulted in several papers (Squires and Eaton, 1989, 1990, 1991a,b,c, 1994). Earlier, Riley and Patterson (1974) had tracked inertial particles in low Reynolds number turbulence simulations to compute Lagrangian statistics. By the late 1980s, DNS codes for simple flows were well established, and adequate supercomputing resources were available to allow tracking a large number of particles. Several efforts started in parallel with our own work. Yeung and Pope (1989) obtained Lagrangian statistics by tracking massless particles in DNS simulations and McLaughlin (1989) studied the deposition of fine aerosol particles in simulated channel flow. Elghobashi and Truesdell (1992) examined particle dispersion in decaying isotropic turbulence.

We used the pseudospectral DNS code developed by Rogallo (1981) for simulating homogeneous–isotropic turbulence and homogeneous shear flows. Neither of these flows is statistically stationary which complicated analysis of the results. Therefore, a forcing scheme was adopted which provided a continuous source of energy allowing the isotropic turbulence simulations to reach a statistically stationary state. Particles were treated as points, and characterized only by an aerodynamic time constant. The particles had no volume displacement, so it was impossible for a particle to occupy more than one computational cell. Particles were tracked by integrating the simple particle equation of motion

$$\frac{dv_i}{dt} = \frac{1}{\tau_p}(u_i[X(t),t] - v_i(t) + g\tau_p\delta_{i2}).$$

Here, v is the particle velocity, $u(X(t),t)$ is the fluid velocity at the position of the particle, τ_p is the particle aerodynamic time constant, and g is the acceleration of gravity assumed to be oriented in the x_2 direction. This implies a linear drag law that is appropriate for small particles at low Reynolds numbers.

With the assumptions above, there are only two issues to consider; the interpolation of the fluid velocity field to the particle position at each time step, and the numerical time advancement of the particle equations of motion. We chose to use second-order accurate Runge–Kutta time advancement for consistency with the Eulerian fluid simulation. Several different interpolation schemes ranging from tri-linear interpolation to fourth order accurate cubic splines and fifth order Lagrange polynomials were tested. There was little effect of the interpolation scheme on the resulting Lagrangian statistics, and third order Lagrange polynomials were used for all the main runs. Yeung and Pope (1989) made a more extensive study of interpolation schemes and arrived at a similar conclusion. Using the simple interpolation schemes, the particle tracking used only a small fraction of the total computing resource. Therefore, it was possible to track large numbers of particles. Numerical experiments were performed in which many sets of particles (each containing 4096 independent particles) were run simultaneously.

The unique aspect of Squires work was the implementation of two-way coupling using an adaptation of Crowe's PSIC method to a 3D, time-dependent simulation. For an incompressible, Newtonian fluid laden with point particles the equations of motion are:

$$\frac{\partial u_i}{\partial x_i} = 0$$

$$\frac{\partial u_i}{\partial t} + \frac{\partial u_i u_j}{\partial x_j} = \frac{-1}{\rho}\frac{\partial p}{\partial x_i} + \nu\frac{\partial^2 u_i}{\partial x_j \partial x_j} - \frac{1}{\rho}f_{pi}$$

where f_{pi} is the local force applied by the fluid onto the particles, ρ is the fluid density, and the effects of gravity have been neglected. It is important for later discussions to realize that there is a significant problem with interpretation of this equation. Under the point-particle assumption, f_{pi} should be zero everywhere except for a delta function at the location of each particle. Generally, this has been interpreted as a smooth continuous function that is a filtered version of the actual point-force distribution. However, the filtering has not been done explicitly.

Our implementation involved computing the force on every particle at every time step of the simulation. The force on each particle was interpolated back to the eight grid points surrounding the particle using a volume-weighting method. The effects of all particles were summed to give the discrete force field needed to advance the fluid equation of motion. Tracking of a very large number of particles was needed to obtain a reasonably smooth force field. Forced, homogeneous, isotropic turbulence was simulated using either 32^3 or 64^3 collocation points to calculate the fluid velocity field. These cases used 3.73×10^5 and 1 million particles respectively. Thus, on average 30 particles (8×1 million/64^3) contributed to the computed particle force at each point for the 64^3 cases. Simulations were done for 10%, 50% and 100% mass loading ratio, and two different particle-time constants. All cases showed significant attenuation of the turbulent kinetic energy. For 100% mass loading and a particle aerodynamic time constant of 0.15 times the turbulence integral scale, a 47% reduction in the turbulent kinetic energy was observed. The turbulence attenuation was similar to reductions observed in some experiments. However, the results could not be directly compared to experiments because there is no precise physical analog to forced homogeneous, isotropic turbulence. The turbulence energy spectra showed broad attenuation in the energy-containing range, and substantial augmentation in the high wave number range. Similar behavior has been observed in many subsequent experiments and simulations. However, in most experiments there is mean relative motion between the particle and fluid phases due to gravity, and it is often assumed that this is responsible for energy input at small scales. The mean velocity for both phases was zero in our simulations, so the augmentation at small scales can only be due to local non-uniformity of the coupling force term.

The large number of particles tracked in the two-way coupled simulations allowed us to accurately resolve the instantaneous particle concentration distribution. This allowed us to observe preferential concentration of particles by turbulence (Squires and Eaton, 1990, 1991c) in which particles with aerodynamic time constants near the Kolmogorov time scale were found to have very high concentrations in localized regions of the turbulence. Maxey (1987) had previously predicted this analytically, and our study allowed quantitative assessment of the degree of concentration as a function of time constant. The simulations also allowed analysis of

specific turbulence structures where particles were concentrated. The highest particle concentrations were found in "convergence zones" as defined by Hunt et al. (1987). Interestingly, this result was initially discounted by referees as being caused by the forcing scheme. Preferential concentration has subsequently been observed in a large number of simulations and experiments (see review by Eaton and Fessler, 1994).

3. Experimental observations of turbulence attenuation

Although this paper is primarily about numerical simulations, it is important to understand the context in which new simulation techniques were developed. Therefore, this section contains a brief summary of a series of experiments conducted in our laboratory specifically to examine turbulence attenuation by dispersed fine particles in gas flows. These experiments were preceded by several studies in turbulent pipe flow by Lee and Durst (1982), Tsuji and Morikawa (1982), and Tsuji et al. (1984) which showed that carrier phase turbulence properties could be changed markedly by dispersed particles even in very simple flows. Rogers and Eaton (1990, 1991) studied turbulence attenuation in a boundary layer developing on the wall of a vertical air wind tunnel laden with 70 μm diameter copper beads at 20% mass loading ratio ($\dot{m}_p/\dot{m}_{air}$). The particle diameter was approximately 1/2 of the estimated Kolmogorov scale. Gas-phase velocity statistics were measured using laser-Doppler anemometry with signal intensity discrimination. The gas-phase mean velocity profiles were unchanged by the presence of particles to within measurement uncertainty. There was roughly a 20% reduction in the turbulence intensity for the inner half of the boundary layer, and augmentation in the outer half where the single-phase turbulence was very small. Power spectra of the streamwise velocity fluctuations showed attenuation at large scales and augmentation at small scales, in agreement with the homogeneous flow simulations.

Kulick et al. (1994) studied a fully developed channel flow with a wider variety of particle sizes and mass loadings. A two-component LDA system was used with a somewhat more robust particle discrimination scheme than Rogers' work. The lightest particles were 50 μm diameter glass beads with a Stokes number of $St = 0.18$ where $St = \tau_p/\tau_f$ and τ_f is k/ε on the channel centerline. The heaviest particles were 70 μm Copper beads with $St = 0.93$. In all cases, the gas-phase mean velocity profile was not changed by the addition of particles. There was only minimal turbulence attenuation for the $St = 0.18$ particles and very strong attenuation for $St = 0.93$ as seen in Fig. 1. At 80% mass loading ratio, the turbulence was essentially eliminated near the channel centerline. Note that all realistic error sources for the LDA measurements would result in measuring the turbulence intensity too high. Measurements of the wall-normal turbulence intensity corroborated these results.

Fessler and Eaton (1999) extended the work to separated flows by adding a backward-facing step to the channel flow apparatus used by Kulick. Three different particle classes were used with mass loading ratios varying from 3% to 40%. Strong attenuation of turbulence was observed at the heaviest loading in the channel upstream of the step. However, the turbulence in the separated shear layer was unaffected by the particles. It was concluded that the strong production in this flow overwhelmed extra dissipation due to particles.

Paris and Eaton (2001) returned to the channel flow to examine the turbulence modification in more detail using particle-image velocimetry (PIV). He used two classes of particles: 70 μm copper with an aerodynamic time constant of 89 ms and 150 μm glass with a 94 ms time constant. The idea was to have two particle classes with roughly the same Stokes number but Reynolds number differing by a factor of 2. Extensive measurements on the channel

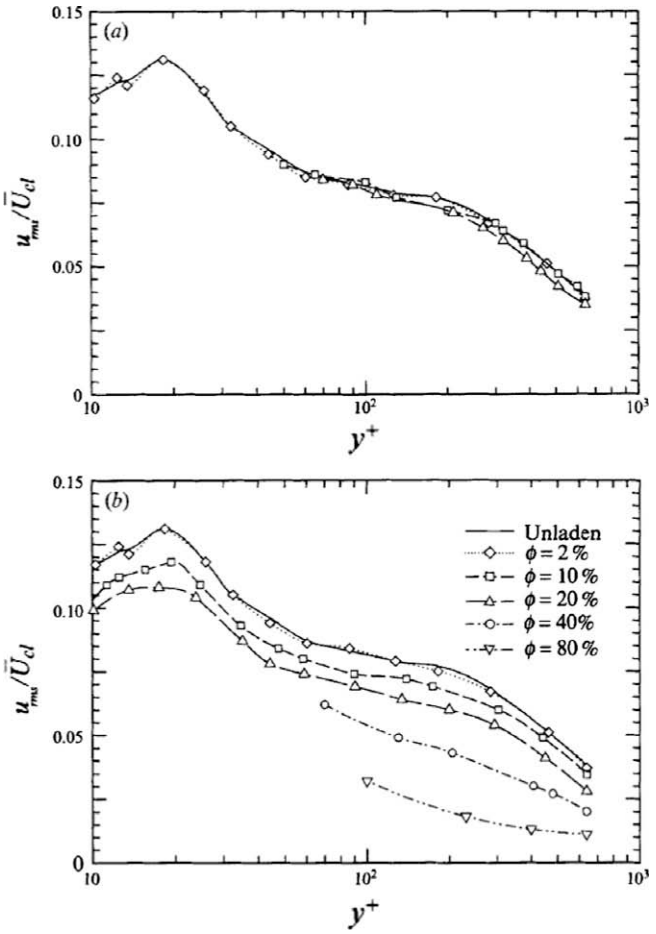

Fig. 1. Streamwise turbulence intensity data for the fully developed channel flow with $St = 0.18$ (top) and $St = 0.93$ (bottom). From Kulick et al. (1994).

centerplane showed strong attenuation of the turbulence in close agreement with Kulick's data. The spanwise turbulence intensity showed similar levels of attenuation. A surprising finding from this work was that the turbulence attenuation was dependent on the particle Reynolds number; significantly greater attenuation was observed with the 150 μm glass particles. This feature of the data could not be captured by a point-particle model in which the only parameter affecting the coupling term is the particle-time constant. In retrospect, it might be expected that the turbulence attenuation would depend on the particle diameter. The Kolmogorov scale at the channel centerline was 160 μm, approximately equal to the diameter of the larger particles. This is a critical point that bears further discussion. In most experiments where large attenuation has been observed, the particle diameter has been of the same order as the Kolmogorov scale. Therefore, it is not sufficient to represent the effects of particles as a smoothly varying force field generally opposing the turbulent motion. The effects of no-slip and impermeability on the surface of finite volume particles must also be considered to understand how particles modify turbulence. We will return to this topic in the following section.

Seeking an even simpler flow, Hwang and Eaton (2006a,b) examined turbulence attenuation in homogeneous–isotropic turbulence in an enclosure. The turbulence was forced by eight synthetic jets in the corners of the enclosure to achieve statistically stationary flow. Glass beads of 165 μm diameter were dropped through the flow falling roughly at their terminal velocity. The particle diameter was very close to the Kolmogorov scale of the single-phase turbulence. Mass loadings of up to 30% were achieved.

Measurements were made using PIV with phase discrimination to allow measurement of the velocity of both phases. Particles falling at their terminal velocity transfer their gravitational potential energy to the fluid velocity. In an enclosed chamber with no net flow, all that energy must go into the velocity fluctuations and eventually be dissipated by viscosity. Therefore, there is a significant additional source of turbulence energy besides what is produced by the synthetic jets. Despite that additional energy input, the turbulent kinetic energy was attenuated by 35 to 40% at a 30% mass loading. The PIV system was used to measure the turbulent kinetic energy dissipation rate. This system did not resolve the flow around individual particles so the full viscous dissipation could not be measured in the particle-laden case. The "resolved dissipation rate" that is the dissipation rate that was estimated by the PIV system actually decreased by 40–50%. This indicates that a large fraction of the total dissipation rate for the multiphase flow actually occurs in the small scale motions surrounding individual particles.

An attempt was made to remove the effects of the relative velocity between the particles and fluid by flying the entire apparatus in NASA's KC-135 microgravity aircraft. There were many experimental difficulties, and the maximum mass loading ratio obtained was only about 8%. The turbulence kinetic energy data had fairly large uncertainty, but the measurements indicated stronger turbulence attenuation in the microgravity case, as would be expected.

4. Simulation difficulties with realistic particle parameters

By the mid 1990s, several different groups were using DNS codes with point-force momentum coupling to explore turbulence modification in various homogeneous turbulent flows. However, there had not yet been any attempts to make direct comparison to experiments. The experimental work discussed above and other parallel studies raised some difficult questions for the simulations. First, as pointed out in Section 3, the strongest attenuation of turbulence was found when particle diameters were of the same order as the Kolmogorov scale of the turbulence.[2] Direct numerical simulation codes for single-phase flows have spatial resolution finer than the Kolmogorov scale. Therefore, particles of realistic size would be partially resolved on a DNS grid. Typically the grid would not be fine enough to fully resolve the flow around an individual particle, but the particles would be too large to reasonably represent as a point. A major problem is then how to capture the effects of the particles on the flow. The particles are large enough to distort actual turbulent eddies. The no-slip and impermeability conditions on the particle surface play a role in modifying the turbulence. The point-force representation can only capture these effects when the particles are much smaller than the Kolmogorov scale.

The second issue is that many problems of interest are for dilute particle-laden flows. The inter-particle spacing may be 10 particle diameters or more. A common situation would have the grid resolution of the DNS being the same as the particle diameter. In that case, most grid cells would not contain any particles, and the particle force field applied onto the fluid would be very "spotty". This is much different than the smoothly varying particle force field which is obtained using the PSIC method with many more particles than grid cells as discussed in Section 2.

A final issue is that the strongest attenuation was observed in wall-bounded turbulent shear layers, namely pipes, channel flows, and boundary layers. Most experiments on free shear layers found only negligible changes to the turbulence. Wall bounded flows create extra difficulties for numerical simulations because of the very high grid resolution required near the wall. For example, the viscous length scale ($l_v = \nu/u_\tau$) for the channel flow experiments of Kulick et al. was approximately 30 μm, less than half the diameter of the particles that created the strongest attenuation. Furthermore, the computational grids near the wall are highly anisotropic to account for elongated near-wall turbulence structures. For example, the computational grid for a channel flow DNS typically has spacing of less than l_v normal to the wall, around $5l_v$ in the spanwise direction, and around $10\,l_v$ in the flow direction. It is hard to rationalize point-force momentum coupling on such a grid.

5. Channel flow simulations

There have been numerous efforts to simulate particle-laden channel flows because of the availability of experimental data sets including those reported above and similar studies by Kussin and Sommerfeld (2002) and Benson et al. (2005). Also, the widespread availability of single-phase DNS and LES codes for the planar channel geometry made this an easy flow for testing two-phase extensions. The present paper will focus on my group's work in this area. There have also been notable contributions by Wang and Squires (1996), Yamamoto et al. (2001) and Portella and Oliemans (2003) who all used various implementations of the point-force coupling scheme.

Rouson (see Rouson et al., 1997; Eaton and Rouson, 1998; Rouson and Eaton, 2001) added Lagrangian particle tracking to the Fourier–Chebyshev spectral channel flow DNS code developed by Kim et al. (1987). This code made explicit use of the particle diameter in both its one-way and two-way coupling implementations. For one-way coupling, the particles rebounded elastically from the wall when they came within one particle radius of the surface. Simulations were set to match the dimensionless particle parameters from Kulick's experiment, but at a lower Reynolds number. Two-way coupling was first implemented using the standard point-force coupling algorithm in which each particle's force is distributed to the eight grid points surrounding the particle center, despite the fact that the particle diameter was greater than grid resolution. This simulation had a one-to-one correspondence between simulated and real particles. In other words, the number of particles in the simulated domain was exactly the same as the number in the experiment. This required 124,400 particles for a 20% mass loading ratio in a domain $2h$ high, $4\pi h/3$ wide, and $4\pi h$ long where h is the channel half width. Thus, there was only 1 particle for every 17 collocation points in the $128 \times 128 \times 129$ grid. The computed results showed negligible changes to the turbulence, in sharp contrast to the experiments. There were small increases in some turbulence components leading to the conclusion that the highly non-uniform particle force distribution was incorrectly enhancing the turbulence.

A second coupling method dubbed the perturbation-field scheme was developed to spread the particle force more realistically through the field. The particle positions were tracked as before using a simple empirical drag law. The back effect force was distributed using a two-term asymptotic expansion for low Reynolds number flow around a sphere. This expansion had both the correct near and far-field behavior. This expansion gave a quasi-steady perturbation velocity field around each particle in spherical coordinates and was evaluated at each time step of the simulation. The velocity perturbation field was transformed to Cartesian coordinates, and the force applied by the particle onto the fluid was evaluated as: $\tilde{f}_i = \tilde{u}_j \partial \tilde{u}_i / \partial x_j$. In other words, a force was applied that would produce the correct velocity perturbation around the particle in steady flow. The force was applied to each grid point

[2] It is important to note that the most widely cited experiments on turbulence attenuation have all been conducted with velocity scales in the range of 10–50 m/s and large scale length scales of the order of 10–50 mm. Thus, the available data encompass a fairly narrow range of Reynolds number. Therefore, it is impossible to determine if it is correct to scale the particle diameter by the Kolmogorov scale, or if turbulence attenuation would even occur at higher Reynolds number.

within 20 radii of a particle's center. This method implicitly assumes that the velocity disturbance field around each particle responds more quickly than turbulent time scales. This assumption is probably not valid for many cases, but the approach does have the advantage that it distributes the total particle force over a spatial domain that is chosen based on quantitative analysis rather than for ease of numerical implementation. Unfortunately, the perturbation-field scheme is extremely compute intensive due to repeated coordinate transformations required to calculate the force field and apply it onto the Cartesian grid. Over 95% of the CPU time was used in calculating the particle force term, and the simulations were never able to run long enough to reach a statistically stationary state.

The Rouson point-force coupled simulations did not reproduce the degree of attenuation observed in the Kulick and Paris channel flow experiments. However, because a direct numerical simulation was used, the computed Reynolds number was almost five times less than the experiment (2793 vs. 13,800). Segura et al. (2004) attempted to rigorously evaluate the capability of particle-laden large eddy simulation by direct comparison to the channel flow experiments of Paris and Eaton (2001) and Benson et al. (2005). This work proceeded in a series of steps. The LES grid and the sub-grid model were carefully adjusted until there was excellent agreement between the simulation and single-phase experiments. Next, passive particle tracking was added including the effects of particle dispersion by sub-grid scale turbulence. The sub-grid model parameters were adjusted to give good agreement between the measured and simulated particle velocities. Finally, point-force two-way coupling was added.

The single-phase, channel flow LES code used as a starting point was developed by Pierce and Moin (2001). It used second-order discretization on a staggered grid, second-order time advancement, and the Germano et al. (1991) dynamic sub-grid scale model. The computation domain size was $2\,h \times 3\,h \times 6\,h$ and a 128^3 grid was used. The Reynolds number based on the friction velocity and the channel half height was $Re_\tau = 644$ to match the experimental conditions. The simulated mean velocity profile and turbulence statistics were compared to the experiments and also to DNS results from Moser et al. (1999). Agreement with the DNS was excellent. There was also excellent agreement with the data of Paris except for some deviation from the turbulence statistics very near the wall ($y^+ < 10$.) The simulated turbulence data were also compared to the highly resolved near-wall data measured by DeGraaff and Eaton (2000). Agreement was within a few percent.

Lagrangian particle tracking used an empirical steady flow drag law to calculate the force applied to each particle. The fluid velocity was interpolated to the center of each particle using tri-linear interpolation. Particle dispersion due to sub-grid scale turbulence was accounted for using a stochastic model for the fluctuating fluid velocity following the work of Oefelein (1997). This method assumes that the sub-grid scale motions are isotropic and have a Gaussian probability density function, with a variance determined by the sub-grid scale kinetic energy. The particle position was advanced using second-order implicit integration, consistent with the flow solver. The time step for the integration was the minimum of the fluid time step, the particle aerodynamic time constant, and an eddy interaction time. The eddy interaction time was an estimate of the amount of time a particle would interact with a given sub-grid scale eddy. This interaction time was the minimum of an eddy lifetime estimated using simple scaling arguments and the time it would take a particle to traverse a typical sub-grid scale eddy. If the relative velocity between the particle and fluid was large, then the traverse time would control the interaction time. If on the other hand, the particle was moving at a velocity close to the resolved fluid velocity, the eddy lifetime would be important. There was one adjustable constant in the model for the sub-grid scale turbulent kinetic energy, which was approximated following Yoshizawa (1984) as:

$$k_{sgs} = 2C_i\Delta^2|\bar{S}|^2$$

where Δ is the LES filter width, $|\bar{S}|^2$ is the norm of the filtered strain rate tensor, and C_i is an adjustable constant. Values of C_i from 0.001 to 0.1 were tested with $C_i = 0.001$ corresponding to essentially no sub-grid scale dispersion model. It was found that the model had a weak effect on the particle mean velocity, as shown in Fig. 2a. Excellent agreement with data was found for $C_i = 0.1$, while there were minor discrepancies near the wall for lower values of C_i. On the other hand, the sub-grid scale dispersion model had a very significant effect on the rms particle velocity in the central part of the channel as shown in Fig. 2b. This result is surprising at first because even with $C_i = 0.1$, the sub-grid scale TKE is less than 1/1000 of the total TKE near the channel centerplane. The increase of the particle rms velocity with increasing C_i is a secondary effect of the sub-grid scale dispersion. Close to the wall, the sub-grid scale TKE is a significant fraction of the total TKE, and the sub-grid scale dispersion acts to increase particle motion normal to the wall. This moves slow moving particles from near the wall into the channel centerplane region thereby increasing the variance of the particle velocity.

Given the excellent agreement of the one-way coupled simulations with experiments with the identical dimensionless parameters, Segura et al. (2004) attempted a two-way coupled simulation using the point-force approach. With the staggered grid discretization used by the flow solver, forces are applied at the cell

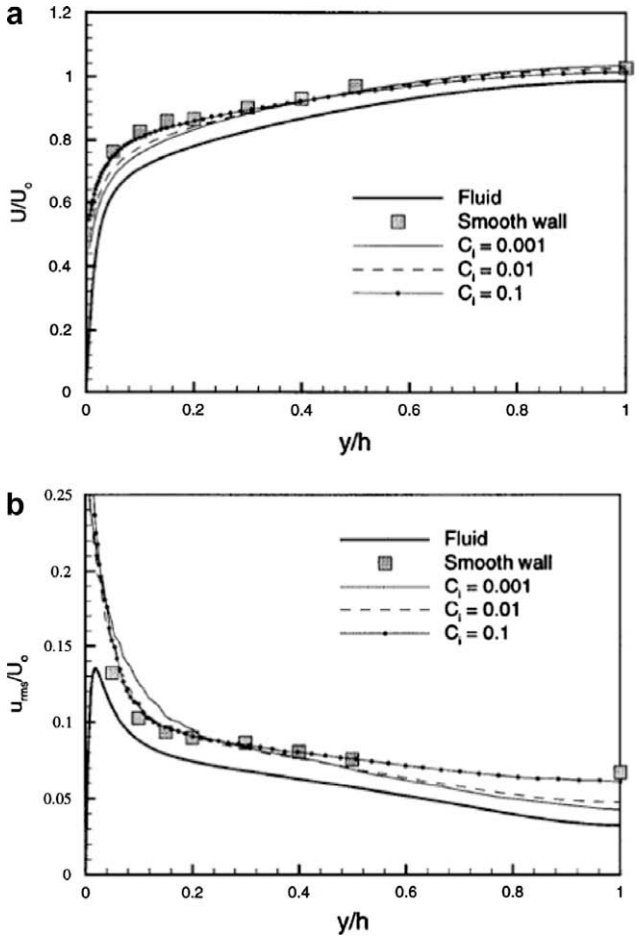

Fig. 2. Large eddy simulation results from Segura et al. (2004) compared to the experiments of Benson et al. (2005). Excellent agreement is seen when the sub-grid scale dispersion model constant is set to 0.1. Plots from Segura et al. (2004).

center. Therefore, the particle force applied for each computational cell was computed as:

$$\vec{F}(\vec{x},t) = \frac{1}{\rho}\frac{1}{V_{\text{cell}}}\sum_{p} m_p \frac{d\vec{u}_p}{dt}.$$

The particle accelerations were calculated in the same way as the one-way coupled simulations, both with and without the sub-grid scale dispersion term. No modifications were made to the gas-phase sub-grid scale model. The dimensionless parameters were chosen to match the experiments of Paris and Eaton (2001) for mass loading ratio of 0.2. A total of 20,000 particles were tracked giving a one-to-one correspondence between experimental and computational particles. This amounted to an average of slightly less than 0.01 particles per computational cell. Fig. 3 shows the streamwise and wall-normal rms fluid velocities for the experiment, for the one-way coupled simulation, and for two way coupled cases with and without the sub-grid scale dispersion model. Although not shown here, the single-phase results were in excellent agreement with the experiments as discussed previously. The discouraging fact is that the two-way coupled simulations show only very minor turbulence attenuation, in sharp contrast to the data. In an attempt to match the experimental results, Segura et al. arbitrarily increased the number of particles by a factor of ten to obtain a mass loading ratio of 2.0. Fig. 4 shows the streamwise turbulence intensity for this case. The agreement with the experiments for $\varphi = 0.2$ is excellent, and there was similar agreement for the wall-normal component. Unfortunately, there is no physical way to justify increasing the particle count to match the experimental results.

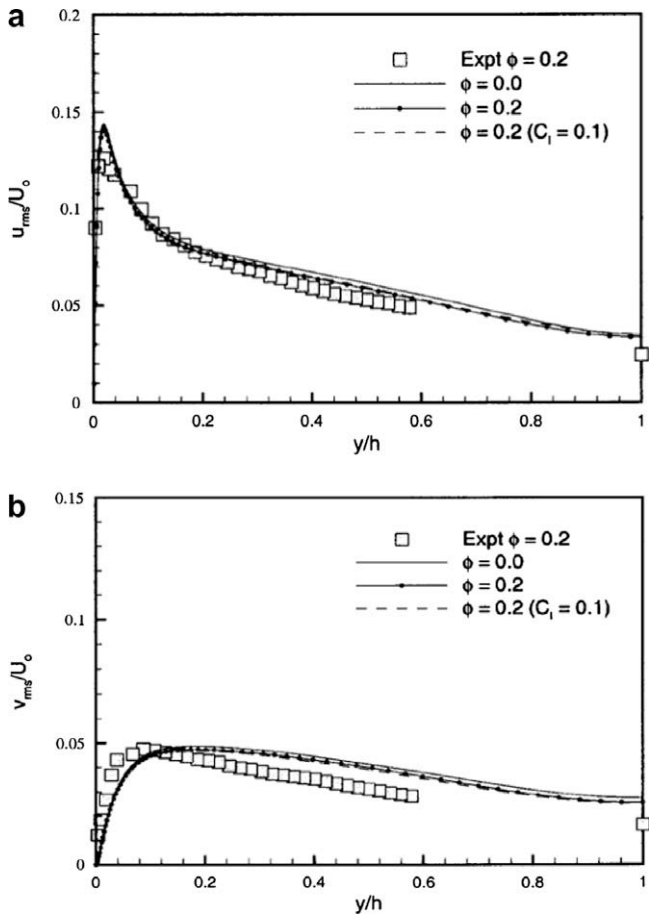

Fig. 3. Fluid turbulence for the channel flow simulations of Segura et al. (2004) and the experiments of Paris and Eaton (2001). (Top) Streamwise turbulence intensity. (Bottom) Wall-normal turbulence intensity. Plots from Segura et al. (2004).

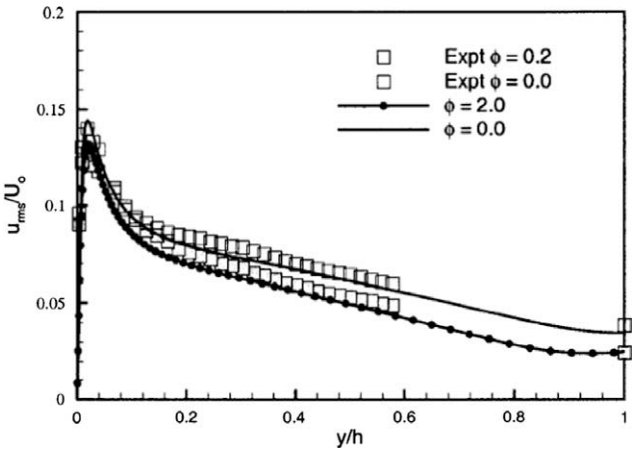

Fig. 4. Streamwise turbulence intensity for the two-way coupled channel flow simulations with 10× too many particles. Plot from Segura et al. (2004).

6. Fully resolved simulations and experiments

Following the careful work of Segura et al. we concluded that point-force coupled numerical simulations were incapable of accurately predicting turbulence attenuation in gas flows. In all cases where significant attenuation has been observed experimentally, the particle diameters are comparable to the smallest scales of the turbulence. Practically, smaller particles with realistic material densities have time constants so small that they essentially follow the flow and apply little net force onto the fluid. Particles much larger than the Kolmogorov scale create substantial unsteady wakes that augment turbulence. When the particles have diameters of the same order as the Kolmogorov scale, the boundary conditions on the particle surface (no-slip and impermeability) are important since turbulent eddies can be distorted by individual particles rather than by the averaged effects of a cloud of particles. Therefore, we concluded that strong turbulence attenuation must at least in part be caused by local dissipation of turbulence around individual particles.

In view of the above conclusions, it is unreasonable to consider a simulation with unresolved particles to be a direct numerical simulation unless the particles are much smaller than the smallest turbulence scales. It is more appropriate to use an explicit large eddy simulation, and absorb the effects of unresolved particles into a sub-grid scale model. However, it is not known how to formulate such a model. Our approach has been to conduct simulations and experiments which resolve the flow around individual particles in order to understand and learn to model the sub-grid scale distortion of turbulence by particles.

The first such effort was the fully resolved simulation of a particle interacting with decaying homogeneous–isotropic turbulence conducted by Burton and Eaton (2005). Bagchi and Balachandar (2003) did highly resolved simulations of frozen turbulence swept past a single fixed particle. These simulations are valuable for understanding how turbulence affects particle motion, but they were not intended for study of turbulence modification. Burton and Eaton (2002) developed an overset grid method in which the local flow immediately around the particle is represented on a highly resolved spherical grid overset on a larger uniform Cartesian grid. Simulations were done for a single fixed particle in the center of a cubic domain with sides of length 192 particle diameters. A $192 \times 192 \times 96$ spherical grid of diameter $70d_p$ captured the flow near the particle. A critical feature of the spherical grid solver was that the results were independent of the flow direction relative to the axis of the spherical coordinates. This is necessary in

turbulent flow calculations, but is not achieved by most spherical coordinates solvers.

The parameters were chosen to mimic typical cases in which strong turbulence attenuation has been observed in experiments. The microscale Reynolds number decayed from 32 to 26 over the course of the simulation. The particle diameter was approximately twice the Kolmogorov length scale, and the particle Reynolds number based on the instantaneous fluid velocity interpolated to the particle center had a maximum value of 19. Since the particle was fixed, the simulation represented particles which are too sluggish to respond to the turbulence. Effectively, the Stokes number was infinite. In most experiments where substantial turbulence attenuation was observed the Stokes number has been quite large, typically between 10 and 100. To obtain useful statistics, a set of 64 independent simulations were run, each with the particle located in a different region of a large turbulence field.

The fully resolved simulations were ideally suited to analyze the local turbulence modification around individual particles in a dispersed flow. Fig. 5 shows the turbulent kinetic energy averaged in spherical shells around the particle and ensemble averaged over the 64 cases. After a short initial adjustment time following the introduction of the particle, the kinetic energy around the particle is attenuated significantly. The TKE is reduced by at least 10% out to a radius of 4–5 particle radii, and there is significant TKE reduction out to at least 10 particle radii. In other words, the local affects of the particle are reducing the turbulence over a fluid volume of at least 1000 times the particle volume. For this single-particle simulation, the volume fraction of particles was only 7.4×10^{-8}, so there is no significant attenuation of the globally averaged turbulent kinetic energy. However, at more typical volume fractions of the order of 10^{-3}, we would expect that these individual particle effects on the turbulence would combine to produce a large global attenuation.

Fig. 6 shows the TKE dissipation rate averaged in shells and ensemble averaged over the 64 simulations. There is a substantial augmentation of the dissipation rate out to $r/d_p = 2$. This is due to the high shear caused by the no-slip condition on the particle's surface, and additional strain caused by the distortion of turbulent eddies around the finite size particle. The high local dissipation is confined to a region which is smaller than the region of significant turbulence attenuation. Apparently, turbulence energy diffuses into the region adjacent to the particle where it is destroyed by the high dissipation rate. We cannot expect to resolve this high dissipation region in a many-particle simulation. Therefore, sub-grid models are needed which produce high dissipation surrounding each particle. High resolution, single-particle simulations are needed for a range of particle and flow parameters to help develop appropriate models.

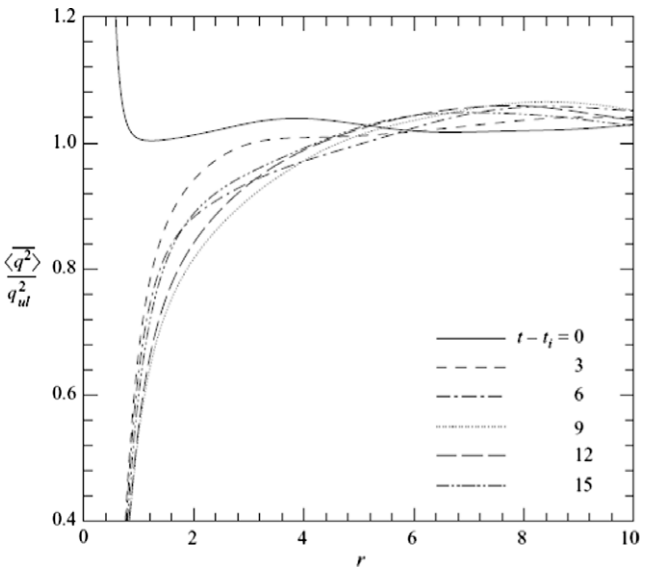

Fig. 5. Ensemble average of the volume average turbulent kinetic energy around the particle at various non-dimensional times following introduction of the particle. The radial coordinate in non-dimensionalized by the particle diameter. Figure from Burton and Eaton (2005).

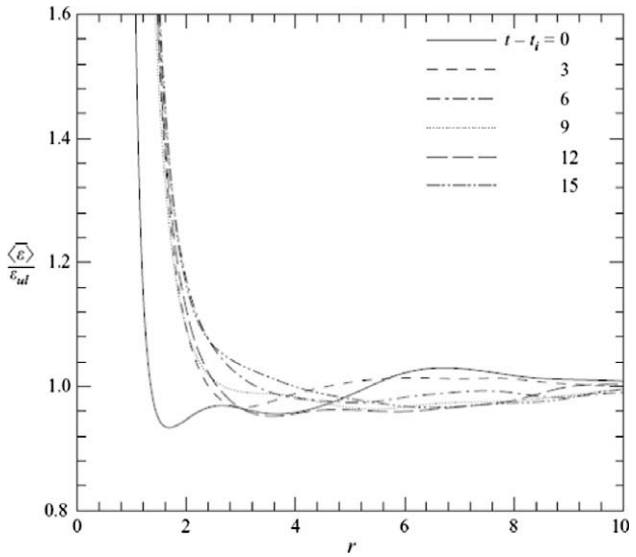

Fig. 6. Ensemble average of the turbulent dissipation rate. Figure from Burton and Eaton (2005).

These results show the critical role that the local distortion of turbulence due to the boundary conditions on individual particles plays in attenuating turbulence. For the regime in which particle diameters are similar to the small scales of the turbulence, the particles act as local sinks of turbulent kinetic energy. In view of these results, it is not surprising that the turbulence attenuation in the channel flow experiments was dependent on particle Reynolds number.

The fully resolved simulations were also used to assess the accuracy of standard Lagrangian particle tracking algorithms by comparing the actual force applied on the particle to the force calculated using various approximate models. Unladen simulations starting from identical initial conditions were run for each case to provide the fluid velocity and time derivatives of the velocity at the location of the particle center. The modeled force was calculated using a semi-empirical particle equation of motion with a history kernel developed by Kim et al. (1998). Only the drag force was found to be significant, in agreement with results from Kim et al. (1998) and Bagchi and Balachandar (2003). The rms force magnitude calculated by the models was between 15% and 30% lower than the actual rms force. This indicates that the Lagrangian tracking methods would underestimate the particle accelerations (at least for this parameter range). Burton and Eaton (2005) concluded that a stochastic model applying an additional fluctuating force to each particle would be the best way to correct for this deficiency in LES type codes. It is also important to note that the underprediction of the fluctuating force would also lead to an underestimation of the back effect of the particles on the turbulence.

Tanaka and Eaton (2007a,b) conducted similar high-resolution studies of particle/turbulence interaction using high-resolution PIV in the homogeneous/isotropic turbulence apparatus developed by Hwang and Eaton (2004). The forced isotropic turbulence had a

microscale Reynolds number of 127 and a Kolmogorov length scale of 110 μm. Three sets of particles were used, 250 μm diameter polystyrene, 250 μm glass and 500 μm glass. The Stokes numbers based on the Kolmogorov time scale ranged from 138 for the polystyrene to 550 for the 500 μm glass, so the particles essentially fell straight through the turbulence. Particle Reynolds numbers based on their terminal velocity ranged from 17 to 130. Measurements were made with a very high resolution, 2D PIV system with velocity vector spacing of 60 μm. A new algorithm was developed to compute the turbulent dissipation rate (Tanaka and Eaton, 2007a) that makes use of the high resolution to produce much more accurate dissipation measurements than were previously possible.

The measurements showed reductions of 10–20% in the turbulent kinetic energy for mass loading ratios near 0.45. We believe that this relatively small reduction is due to the fact that the particles were substantially larger than in the previous experiments. Unsteady wakes of the falling particles were a significant source of turbulence, but this was overcome by extra dissipation around particles. One of the most interesting results regarded the TKE dissipation rate. Similar to the numerical results of Burton, a substantial augmentation of the dissipation rate was observed around the particles, as shown in Fig. 7. This figure was obtained by ensemble averaging the measured dissipation around every particle found in the 5000 image pairs of PIV data. The dissipation rate is augmented by up to a factor of 3 near the particle. This effect is quite asymmetric; the dissipation is much higher on the bottom side. It is not clear why this occurs, but it is important to note that the particle is falling in the negative x_2 direction. The dissipation averaged over the entire field remained almost constant with the addition of particles as seen in Fig. 8. The extra dissipation around the particles made up for a small reduction in the dissipation elsewhere. This result is in sharp contrast with previous under-resolved PIV dissipation measurements and point-force coupled DNS calculations, neither of which can resolve the local flow around the particles. Fig. 8 also shows estimates from a simple model proposed by Tanaka and Eaton (2007a,b):

$$\varepsilon_{\text{laden}} = \varepsilon_o + \frac{\Delta K}{\tau_p}.$$

where ε_o is the dissipation rate without particles, ΔK is the change in turbulence kinetic energy, and τ_p is the particle-time constant.

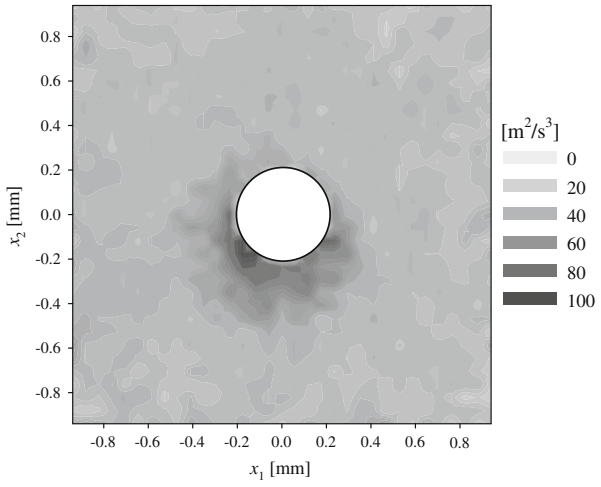

Fig. 7. Ensemble average turbulent dissipation (in m^2/s^3) around 500 μm particles in isotropic turbulence. Figure from Tanaka and Eaton (2007a,b).

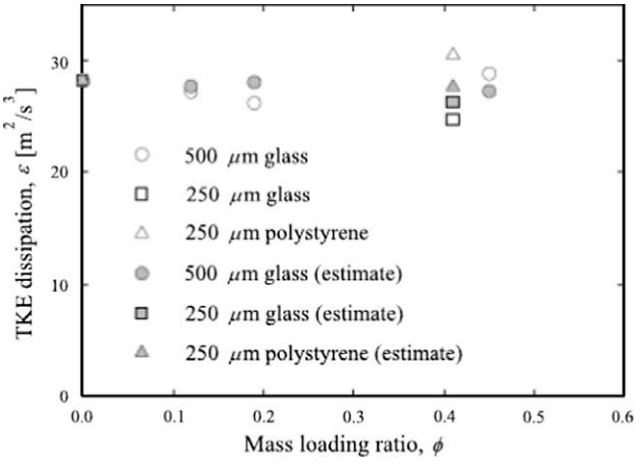

Fig. 8. Average dissipation rate for particle-laden isotropic turbulence. Figure from Tanaka and Eaton (2007a,b).

7. Future work in point-force coupled simulations

Simulations of gas flows laden with dilute loadings of solid particles or liquid droplets will play a major role in understanding, analyzing, and designing many critical multiphase flow systems. Techniques of Lagrangian particle tracking within Eulerian DNS and LES codes have become very well established since their initial development in the late 1980s. As computer resources continue to expand and LES codes become more efficient and user friendly, their use in the analysis of systems such as spray combustors will become commonplace. Already, simulations have been used to discover preferential concentration of particles in flows, where it was later found experimentally. However, in my opinion we are not proceeding with due caution. Highly resolved simulations show that the commonly used models are not adequate for tracking particles at least for some range of particle parameters. More work of this sort is needed to delineate the range of validity of the models.

Two-way coupled Eulerian–Lagrangian simulations using the point-force technique have not fulfilled their early promise. This paper, and my work in general have focused on a range of particle parameters where turbulence modification can be very significant. This range encompasses a wide variety of technological and natural flows. In my opinion, various implementations of point-force coupling are being used without proper acknowledgement of the method's shortcomings. Careful tests of the method have shown that it cannot capture experimentally observed turbulence attenuation. Furthermore, recent fully resolved simulations and high-resolution measurements show that the local flow around the particles is critical. It may be that these conclusions are particular to one special flow regime. However, I believe it is incumbent on the developers of these codes to prove that the models are valid, either through fully resolved simulations, or direct comparison to experiments.

The high-resolution experiments and simulations indicate that the local flow around individual particles is important to the overall flow development. Simulations by Bagchi and Balachandar (2003) and Burton and Eaton (2005) have shown that very high grid resolution is required to capture particle-turbulence interaction. Resolution of the flow around hundreds of thousands of particles in a flow field is beyond hope. Therefore, modified versions of point-force coupling are needed. I believe that the appropriate approach is to use LES with a sub-grid scale model that is locally modified by particles. Development of such a model will have to be guided by a large set of fully resolved simulations.

Acknowledgements

I am deeply indebted to a long line of outstanding Ph.D. students who have worked with me in particle-laden gas flows. These include Sunil Kale, Chris Rogers, Kyle Squires, Ellen Longmire, Jonathan Kulick, Ryan Wicker, John Fessler, Damian Rouson, Tony Paris, Judith Segura, Tristan Burton, Wontae Hwang, Tomohiko Tanaka, and Michael Benson. Dr. Joseph Oefelein, although not a member of my group also contributed immensely to our modeling efforts.

References

Bagchi, P., Balachandar, S., 2003. Effect of turbulence on the drag and lift of a particle. Phys. Fluids 15, 3496–3513.
Benson, M., Tanaka, T., Eaton, J.K., 2005. Effects of wall roughness on particle velocities in a turbulent channel flow. Trans. ASME. J. Fluids Eng. 127, 250–256.
Burton, T.M., Eaton, J.K., 2002. Analysis of fractional-step method on overset grids. J. Comput. Phys. 177, 336–364.
Burton, T.M., Eaton, J.K., 2005. Fully resolved simulations of particle-turbulence interaction. J. Fluid Mech. 545, 67–111.
Crowe, C.T., Sharma, M.P., Stock, D.E., 1977. The particle-source-in cell (PSI-CELL) model for gas-droplet flows. Trans. ASME J. Fluids Eng. 99, 325–332.
DeGraaff, D.B., Eaton, J.K., 2000. Reynolds number scaling of the flat plate turbulent boundary layer. J. Fluid Mech. 422, 319–346.
Eaton, J.K., Fessler, J.R., 1994. Preferential concentration of particles by turbulence. Int. J. Multiphase Flows 20, 169–209.
Eaton, J.K., Rouson, D.W.I., 1998. Particle interaction models for higher order simulations of particle-laden turbulence. In: 3rd Intl. Conf. Multiphase Flow, Lyon, France.
Elghobashi, S., Truesdell, G.C., 1992. Direct simulation of particle dispersion in decaying isotropic turbulence. J. Fluid Mech. 242, 655–700.
Fessler, J.R., Eaton, J.K., 1999. Turbulence modification by particles in a backward-facing step flow. J. Fluid Mech. 394, 97–117.
Germano, M., Piomelli, U., Moin, P., Cabot, W.H., 1991. A dynamics sub-grid-scale eddy viscosity model. Phys. Fluids 3, 1760–1765.
Hunt, J.C.R., Wray, A.A., Moin, P., 1987. In: Proc. CTR Summer Program, pp. 193–208.
Hwang, W., Eaton, J.K., 2004. Creating homogeneous and isotropic turbulence without a mean flow. Exp. Fluids 36, 444–454.
Hwang, W., Eaton, J.K., 2006a. Homogeneous and isotropic turbulence modulation by small heavy ($St \sim 50$) particles. J. Fluid Mech. 564, 361–393.
Hwang, W., Eaton, J.K., 2006b. Turbulence attenuation by small particles in the absence of gravity. Int. J. Multiphase Flow 32, 1386–1396.
Kale, S.R., Eaton, J.K., 1985. Experimental investigation of gas-particle flows through diffusers in the freeboard region of fluidized beds. Int. J. Multiphase Flow 11, 659–674.
Kim, I., Elghobashi, S., Sirignano, W.A., 1998. On the equation for spherical-particle motion: effect of Reynolds and acceleration numbers. J. Fluid Mech. 367, 221–253.
Kim, J., Moin, P., Moser, R.D., 1987. Turbulence statistics in fully developed channel flow at low Reynolds number. J. Fluid Mech. 177, 133–166.
Kulick, J.D., Fessler, J.R., Eaton, J.K., 1994. Particle response and turbulence modification in fully developed channel flow. J. Fluid Mech. 277, 109–134.
Kussin, J., Sommerfeld, M., 2002. Experimental studies on particle behaviour and turbulence modification in horizontal channel flow with different wall roughness. Exp. Fluids 33, 143–159.
Lee, S.L., Durst, F., 1982. On the motion of particles in turbulent duct flows. Int. J. Multiphase Flow 8, 125–146.
Maxey, M.R., 1987. Gravitational settling of aerosol particles in homogeneous turbulence and random flow fields. J. Fluid Mech. 174, 441–465.
McLaughlin, J.B., 1989. Aersol particle deposition in numerically simulated channel flow. Phys. Fluids 1, 1211–1224.
Moser, R.D., Kim, J., Mansour, N.N., 1999. Direct numerical simulation of turbulent channel flow up to $Re_\tau = 590$. Phys. Fluids 11, 943–945.
Oefelein, J.C., 1997. Simulation and Analysis of Turbulent Multiphase Combustion at High Pressures, Ph.D. Thesis. The Pennsylvania State Univ.
Paris, A.D., Eaton, J.K., 2001. Turbulence Attenuation in a Particle-Laden Channel Flow, Report TSD-137, Dept. of Mechanical Engineering, Stanford University.
Pierce, C.D., Moin, P., 2001. Progress-Variable Approach for Large-Eddy Simulation of Turbulent Combustion, Report TF-80, Mechanical Engineering, Stanford University.
Portella, L.M., Oliemans, R.V.A., 2003. Eulerian–Lagrangian DNS/LES of particle-turbulence interactions in wall-bounded flows. Int. J. Numer. Methods Fluids 43, 1045–1065.
Riley, J.J., Patterson, G.S., 1974. Diffusion experiments with numerically integrated isotropic turbulence. Phys. Fluids 17, 292–297.
Rogallo, R.S., 1981. Numerical Experiments in Homogeneous Turbulence. NASA Tech. Memo. 81315.
Rogers, C.B., Eaton, J.K., 1990. The behavior of solid particles in a vertical turbulent boundary layer in air. Int. J. Multiphase Flows 16, 819–834.
Rogers, C.B., Eaton, J.K., 1991. The effect of small particles on fluid turbulence in a flatplate, turbulent boundary layer in air. Phys. Fluids A 3, 928–937.
Rouson, D.W.I., Eaton, J.K., Abrahamson, S.D., 1997. A Direct Numerical Simulation of Particle-Laden Turbulent Channel Flow, Rept. TSD-101, Mechanical Engineering Dept., Stanford University.
Rouson, D.W.I., Eaton, J.K., 2001. On the preferential concentration of solid particles in turbulent channel flow. J. Fluid Mech. 428, 149–169.
Segura, J.C., Oefelein, J.C., Eaton, J.K., 2004. Predictive Capabilities of Particle-Laden Large Eddy Simulation, Rept. TSD-156, Mechanical Engineering Dept., Stanford University.
Squires, K.D., Eaton, J.K., 1989. Study of the effects of particle loading on homogeneous turbulence using direct numerical simulation. In: Michaelides and Stock (Eds.), Turbulence Modification in Dispersed Multiphase Flows, ASME FED, vol. 80, pp. 37–44.
Squires, K.D., Eaton, J.K., 1990. Particle response and turbulence modification in isotropic turbulence. Phys. Fluids A 2, 1191–1203.
Squires, K.D., Eaton, J.K., 1991a. Lagrangian and Eulerian statistics obtained from direct numerical simulations of homogeneous turbulence. Phys. Fluids 3, 130–143.
Squires, K.D., Eaton, J.K., 1991b. Measurements of particle dispersion obtained from direct numerical simulations of isotropic turbulence. J. Fluid Mech. 226, 1–31.
Squires, K.D., Eaton, J.K., 1991c. Preferential concentration of particles by turbulence. Phys. Fluids 3, 1169–1178.
Squires, K.D., Eaton, J.K., 1994. Effect of selective modification of turbulence on two-equation models for particle-laden turbulent flows. J. Fluids Eng. 116, 778–784.
Tanaka, T., Eaton, J.K. 2007a. High Resolution Measurements of Turbulence Modification by Particles, Rept. TF-102, Dept. of Mechanical Engineering, Stanford.
Tanaka, T., Eaton, J.K., 2007b. A correction method for measuring turbulence kinetic energy dissipation rate by PIV. Exp. Fluids 42, 893–902.
Tsuji, Y., Morikawa, Y., 1982. LDV measurements of air-solids two-phase flow in a horizontal pipe. J. Fluid Mech. 120, 385–409.
Tsuji, Y., Morikawa, Y., Shiomi, H., 1984. LDV measurements of air-solids flow in a vertical pipe. J. Fluid Mech. 139, 417–434.
Wang, Q., Squires, K.D., 1996. LES of particle-laden turbulent channel flow. Phys. Fluids 9, 1207–1223.
Yamamoto, Y., Potthoff, T., Tanaka, T., Kajishima, T., Tsuji, Y., 2001. Large eddy simulation of turbulent gas particle flow in a vertical channel: effect of considering inter-particle collisions. J. Fluid Mech. 422, 303–334.
Yeung, P.K., Pope, S.B., 1989. Lagrangian statistics from direct numerical simulations of isotropic turbulence. J. Fluid Mech. 207, 531–586.
Yoshizawa, A., 1984. Statistical analysis of the deviation of the Reynolds stress for its eddy-viscosity representation. Phys. Fluids 27, 1377–1387.